Mon. Not. R. Astron. Soc. **000**, 000–000 (0000) Printed 9 June 1998 (MN LATEX style file v1.4)

Size, Mass and Shape of the Milky Way

Rob P. Olling[1]*, Michael R. Merrifield[1]†
[1] *Dept. of Physics and Astronomy,*
University of Southampton, Southampton SO17 1BJ, U.K.

9 June 1998

ABSTRACT

The shape of the Milky Way's dark halo has been determined using two independent methods. First, we have compared the amount of dark matter close to the Galactic plane as inferred from stellar kinematics to the predictions of the different dark halo models. Second, we have compared the thickness of the Galaxy's gas layer to the predictions of dark halos models with a wide range in halo shape. Combining these two techniques, we find that the Milky Way has a relatively-round dark halo with shortest-to-longest axial ratio of $q = 0.75 \pm 0.25$. The results depend on three somewhat uncertain parameters: 1) the Sun's distance from the Galactic centre (R_0); 2) the Galactic rotation speed at the Solar circle (Θ_0); and 3) the stellar column density in the Solar neighbourhood (Σ_*). We find that an internally consistent Milky Way model can only be constructed for a very limited range in parameters: choosing any two of the four parameters ($R_0, \Theta_0, \Sigma_*, q$), uniquely determines the remaining two.

If we only impose the constraint that dark halo is oblate, we infer that $\Theta_0 \lesssim 188 - 5.6(R_0 - 7) + 4(R_0 - 7)^2$ km s^{-1}. We also find that models using either the IAU-sanctioned Galactic constants of 8.5 kpc and 220 km s^{-1}, or the "current best" values of 7.8 kpc and 200 km s^{-1}, require substantially prolate halos ($q = 1.8$, and $q = 1.6$, respectively), and are hence excluded. Given the strong inter-relations between the parameters of Galactic mass models, the distance to the Galactic centre can be determined in several ways: 1) the observed value of the Σ_* implies $R_0 = 7.3 \pm 0.3$ kpc, and 2) the observed Oort constant combination $A - B$ together with the oblateness constraint for the dark halo yields $R_0 \lesssim 7.2 \pm 0.2$ kpc.

If the Milky Way's rotation speed is larger than $\sim$170 km s^{-1} we can rule out two dark matter candidates that require a highly flattened dark matter halo: 1) decaying massive neutrinos; and 2) a disk of cold molecular hydrogen. In the accompanying paper we show that the above conclusions are not significantly affected by the possible non-thermal pressure support of the gas layer.

These results imply that the luminous Milky Way is smaller than hitherto assumed. Such a leaner Galaxy is entirely consistent with all observational kinematical constraints, including the only geometric determination of R_0 from water maser proper motions (7.2 ± 0.7 kpc), the reflex motion of the Galactic centre, the Oort constants, radial velocities and proper motions of Cepheids, the Hipparcos based determination of the local mass density, the local Galactic escape velocity, the peculiar velocity of M31, and the orbits of the Milky Way satellite galaxies.

Key words: Galaxy: structure - Galaxy: kinematics and dynamics - Galaxy: solar neighborhood - Galaxy: fundamental parameters - Galaxy: stellar content - ISM: general

* E-mail: olling@astro.soton.ac.uk
† E-mail: mm@astro.soton.ac.uk

1 INTRODUCTION

The speed at which spiral galaxies rotate remain relatively constant out to large radii (eg, Rubin, Ford & Thonnard 1980; Bosma 1981), which implies that they contain large amounts of dark matter (DM). The roundest halos –with shortest-to-longest axis ratio of $q = c/a \sim 0.8$ (Peebles 1993)– are predicted by galaxy formation models in which hot dark matter is dominant. Cosmological cold dark matter simulations typically result in triaxial dark halos (Warren *et al.* 1992) while the inclusion of gas dynamics in the simulations results in oblate halos (Katz & Gunn 1991; Udry & Martinet 1994; Dubinski 1994) with $q = 0.5 \pm 0.15$ (Dubinski 1994). Other dark matter candidates produce halos as flat as $q \lesssim 0.2$ (Pfenniger, Combes & Martinet 1994; Sciama 1990). Clearly, the determination of q for real galaxies offers a valuable test for discriminating between these cosmological models. To-date, comparisons with theory are somewhat inconclusive (Olling 1997c; Olling & Merrifield 1997b). The halo flattenings inferred from the warping gas layer method (Hofner & Sparke 1994) stand apart from the other methods (Fig. 1). One possible explanation for this discrepancy is that the dark matter distribution adjust itself to the presence of the stellar components (Dubinski & Kuijken 1995; Nelson & Tremaine 1995; Binney, Jiang & Dutta 1997).Indeed, preliminary analysis of the flaring of NGC 3198 indicate $q \sim 0.5$, rather than the round halo inferred from the warping analysis (Olling, private communications).

To determine the shape of the Milky Way's dark matter halo we need a tracer whose kinematics or distribution depends on the vertical distribution of matter. Large midplane densities are indicative of flattened dark halos, while low densities are the signature of extended (round) DM distributions. The rotation curve [circular speed as a function of radius, $\Theta(R)$] of the Galaxy contains no information about the halo's shape as it probes the potential in one direction only. However, in order to determine the halo's shape, knowledge of the rotation curve is indispensable for two reasons.

First, the properties of an important mass component, the interstellar medium (ISM), depend on the rotation curve. Our location within the Milky Way means that we cannot determine distances to diffuse components like the ISM directly. Instead, we must infer the distance by comparing the observed radial velocity of the material with the predictions of a kinematical model. Thus, important properties like scale-height, column density, and total mass of the ISM depend on the Galactic constants and the Milky Way's rotation curve (see also the accompanying paper, henceforth Paper II).

Second, our location inside the Galaxy means that modest uncertainties in our distance of the Galactic centre [$R_0 = 7.8 \pm 0.7$ kpc (Reid 1993)] and the Galactic rotation speed [$\Theta_0 = 200 \pm 20$ km s^{-1} (Sackett 1997)] result in significant variations in the inferred rotation curves (see Fig. 2, and Olling & Merrifield 1998b). To see how this uncertainty influences the determination of the halo's flattening, imagine the following situation: suppose that the flattening analysis indicates a large DM density and a substantially flattened DM halo. However, such large midplane density can also be attained if we choose a larger value for Θ_0. Such larger rotation speeds imply more dark matter, with a larger midplane DM density. Thus, the same DM density can be obtained with a larger value for Θ_0 and a rounder halo. Therefore, the inferred flattening of the Milky Way's dark matter halo will depend on the adopted amplitude of the rotation curve. Similarly, the inferred halo flattening depends on our distance to the Galactic centre, as most Galactic size and mass scales depend on R_0.

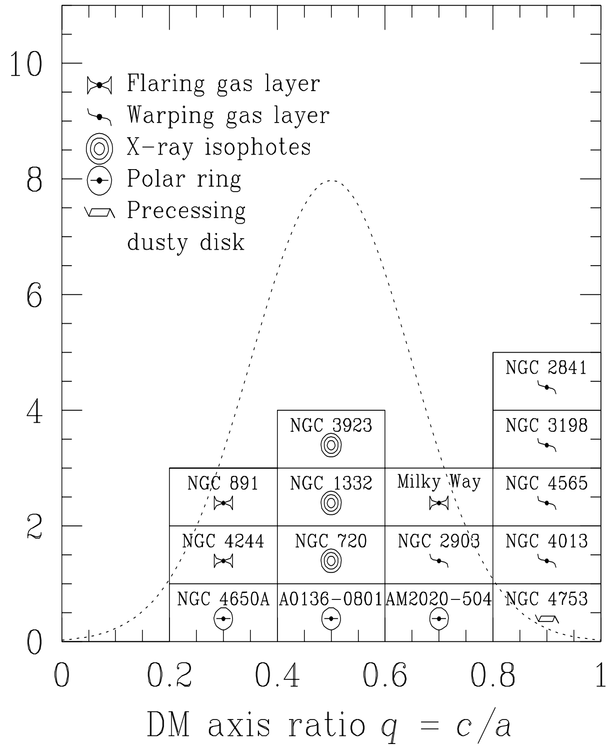

Figure 1. A comparison between the cold dark matter predictions of the dark matter halo shape ($q = 0.5 \pm 0.15$, dotted line; Dubinski 1994) and the observations (histogram). For each individual galaxy we indicate the identification and technique used to determine the halo's flattening: 1) Flaring gas layer (Olling 1996b; Olling & Merrifield 1997b; Becquaert, Combes & Viallefond 1997); 2) Warping gas layer (Hofner & Sparke 1994); 3) X-ray isophotes, (Buote & Canizares 1996, 1998); 4) Polar ring galaxies (Arnaboldi *et al.* 1993; Sackett *et al.* 1994; Sackett & Pogge 1995); 5) precessing dusty disk (Steiman-Cameron, Kormendy, & Durisen 1992).

To determine the shape of the Milky Way's dark matter halo, we can employ two independent methods. First, the manner in which the thickness of the gas layer increases with radius, or "flares", provides a constraint on the shape of the dark matter halo. The thickness of the gas layer is set by a hydrostatic balance between the random thermal motions of the gas and the vertical component of the Milky Way's gravitational field. Thus, the thickness of the layer depends on the detailed distribution of mass in the Galaxy: more mass close to the plane forces the gas into a thinner layer. For any given mass distribution, we can calculate the gravitational force, and thus predict the thickness of the gas layer via the equation of hydrostatic equilibrium (Olling 1995; Olling 1996b). Since the thickness of the stellar disk is much smaller than the scale-height of the dark halo, the shape of the potential close to the plane is strongly affected by the stellar disk. The thickness of the gas layer is sensitive to the shape of the dark matter halo only at radii larger than 4-5 optical scale-lengths where the stellar densities become negligible. Beyond the optical disk, where the potential is dominated by the halo, the details of the stellar mass distribution like scale-length (Dehnen & Binney 1998) or the stellar mass-to-light ratio do not affect the flaring significantly (Olling 1995; Olling 1996b; Paper II). Furthermore, the gas is expected to be in the warm neutral phase beyond the optical disk (§4.2), so that a single isothermal component is sufficient to characterize the ISM.

For the Milky Way, there is another constraint that discriminates between dark halo models. Studies of the motions of stars in the Galactic disk near the Sun imply that the total amount of mass within 1.1 kpc of the Galactic plane is $\Sigma_{1.1}^{tot} = 71{\pm}6\ M_\odot\,\mathrm{pc}^{-2}$ (Kuijken & Gilmore 1991; henceforth KG91). In Paper II we confirm KG91's assertion that the measurement of $\Sigma_{1.1}^{tot}$ is independent of the detailed shape of the density distribution. Furthermore, we show that its value is independent of the assumed Galactic constants. Thus, $\Sigma_{1.1}^{tot}$ provides a robust constraint for Galactic mass models. Just like the gas flaring, this quantity provides a measure of the amount of mass close to the plane, and so it can be used to measure the dark halo's flattening. However, because there is a significant contribution to the value of $\Sigma_{1.1}^{tot}$ from the stellar disk itself, this method *does* depend on the properties of the stellar disk. In particular, it depends on the local stellar column density (Σ_*), which is somewhat uncertain. Estimates for Σ_* range from 25.8 $\pm\, 3.8\ M_\odot\,\mathrm{pc}^{-2}$ (Gould, Bahcall & Flynn 1997; henceforth GBF97) through 35 $\pm$ 5 $M_\odot\,\mathrm{pc}^{-2}$ (Kuijken & Gilmore 1989b; henceforth KG89) to 145 $M_\odot\,\mathrm{pc}^{-2}$ (Bahcall 1984b).

We thus expect that the halo flattening as inferred from the flaring of the gas layer ($q_{\mathrm{H\ I}}$) depends only slightly on the mass of the stellar disk, while the flattening determined from the total amount of matter within 1.1 kpc from the plane ($q_{1.1}$) will show a strong dependence on Σ_*. A particular Milky Way model is only self-consistent if $q_{\mathrm{H\ I}}$ and $q_{1.1}$ are identical. Both $q_{\mathrm{H\ I}}$ and $q_{1.1}$ depend on R_0, Θ_0, and Σ_* as explained above. In fact, the accurate determination of any two parameters from the list (R_0, Θ_0, Σ_*, q) allows for the determination of the remaining two parameters (see below).

In Paper II, we investigate how the poorly-determined gaseous velocity dispersion (σ_g) affects the determination of the equilibrium thickness of the H I layer, and hence the inferred $q_{\mathrm{H\ I}}$ and the other parameters of the mass model. The results indicate only a small dependence on σ_g, so we will not discuss the implications further in this paper.

The plan of this paper is as follows. In Section 2 we present the rotation curve of the Milky Way and indicate the uncertainties in its determination. In §3 we describe the components that make up the mass distribution of the Galaxy. The determination of the thickness of the gas layer is described in §4. In section 4.2 we discuss the state of the ISM beyond the optical disk. In §5 we combine the two flattening constraints. We consider some of the caveats in §6. The implications for the size, mass and shape of the Milky Way are discussed in Sections 7 and 8.

2 THE OBSERVED ROTATION CURVE

When studying the dark halo of the Milky Way, determining its rotation curve is important for two reasons. First, the rotational velocity at any radius is a measure of the total amount of mass inside that radius, and so, after subtracting the contributions from the visible matter and assuming a value for the flattening q, it yields the mass of the dark halo. Second, as explained in the Introduction, it provides the key to locating objects within the Galaxy. Thus, the thickness of the gas layer can only be determined if the Galaxy's rotation curve is known. Unfortunately, although the rotation of the Milky Way has been extensively studied since its discovery almost seventy years ago, its exact form has not been determined unambiguously (for recent reviews, see Fich & Tremaine 1991, Reid 1993, or Sackett 1997). What is most reliably determined is the function $W(R/R_0)$:

$$W\left(\frac{R}{R_0}\right) \quad = \quad \frac{R_0}{R} \times \Theta(R) - \Theta_0 \ , \qquad (1)$$

with R the Galactocentric distance‡ The $W(R/R_0)$ curve has been determined observationally from H I & H_2 tangent points in the inner Galaxy [e.g., (Malhotra 1995; Malhotra 1994)]. Beyond the Solar circle we use methods based on the width of the H I layer (Merrifield 1992) and distances to H II regions (Brand & Blitz 1993). To obtain the rotation curve, one has to know both Θ_0 and R_0, which are less well determined, so we adopt a range of values for the distance to the Galactic centre to allow for this uncertainty (R_0 = 6.8, 7.1, 7.8 and 8.5 kpc). The values of Θ_0 are then set by local stellar kinematic measurements of the Oort A and B constants, which require that $\Theta_0/R_0 = A - B = 26.4 \pm 1.9$ km s^{-1}kpc^{-1} (Kerr & Lynden-Bell 1986), and so we adopt Θ_0 = 182, 189, 207 and 227 km s^{-1}, respectively. The resulting rotation curves for two cases are shown in Fig. 2. We present a larger ensemble of possible rotation curves elsewhere (Olling & Merrifield 1998b). Note that the IAU-recommended values for R_0 and Θ_0 result in a rising rotation curve, which is rarely seen in galaxies of similar Hubble type (Merrifield 1992).

3 MASS MODELS

We must now explain the observed rotation curve in terms of the motion induced by the gravitational pull of both visible

‡ Throughout this paper we use cylindrical coordinates with R the Galactocentric distance and z the distance from the plane.

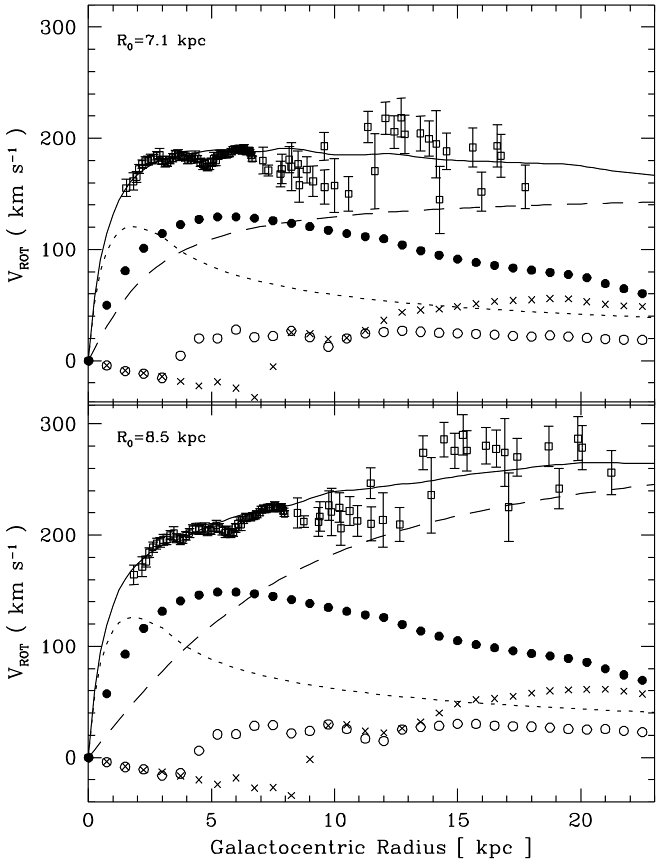

Figure 2. The rotation curve for the Milky Way for the extreme values of R_0 =7.1 and 8.5 kpc (open squares). The figure also shows how the rotation curve can be broken down into the contributions due to: the stellar disk (filled circles); the bulge (dotted line); the H I layer (crosses, negative values mean that the force is directed outwards); the H_2 layer (circles); and the dark halo (dashed line). While fitting disk-halo models, we do not use the data in the inner three kpc since non-circular motions strongly affect the apparent rotation curve (Combes 1991). The best fit model, which is obtained by summing the individual components in quadrature, is shown as a full line.

and dark components. As is customary (e.g., van Albada & Sancisi 1986; Kent 1987; Begeman 1989; Lake & Feinswog 1989; Broeils 1992; Olling 1995; Olling 1996c), we decompose the Galaxy into different mass components: a stellar bulge and disk; an azimuthally symmetric gas disk; and a dark matter halo. For all the R_0-Θ_0 combinations enumerated in the previous Section and a range in stellar mass-to-light ratios, disk scale-lengths ($h_{\rm R}$), and halo flattenings, we calculate fully self-consistent, axi-symmetric, mass models for the Milky Way. These models yield accurate predictions of the hydrostatic equilibrium thickness of the gas layer, which will be compared to the observed widths to yield the halo flattening. A full description of the models is presented in Paper II.

In Fig. 2 we also show how the contributions from the various mass components can be combined to reproduce the observed rotation curve. Clearly, this process alone is not sufficient to choose between different values of R_0 and Θ_0. Further, by adopting different values for the stellar mass-to-light ratios, stellar scale-length, or halo shape, a different balance can be struck between the visible and dark components that matches the observed rotation curve equally well. Thus this analysis tells us little about the radial distribution and shape of the dark halo. In Paper II, we present the inferred radial dark matter distribution, and its dependence on the parameters of the mass models.

4 THE THICKNESS OF THE GAS LAYER

4.1 The observations

As discussed above, distances to H I in the Milky Way, and hence the measured widths of the gas layer depend on the assumed rotation curve for the Galaxy. If material at Galactic coordinates (l, b) has radial velocity v_r, then it must lie at radius R in the Galaxy such that

$$W(R/R_0) \quad = \quad \frac{v_r}{\sin l \cos b} \,. \tag{2}$$

Thus, once $W(R/R_0)$ is a known function, and particular values for R_0 and Θ_0 are adopted, one can infer the Galactocentric radius of the material. Simple geometry shows that

$$R^2 \quad = \quad R_0^2 + d^2 \cos^2 b - 2 R_0 \; d \cos l \cos b \,, \tag{3}$$

where d is the distance to the material. With the thus determined distance, the thickness of the gas layer can be calculated from its measured angular thickness. Thus, for every choice for R_0 & Θ_0, the widths have to be re-determined. Unfortunately, this operation is not a simple scaling, as most widths presented in the literature are averages over a range in Galactocentric azimuth. Altering the Galactic constants changes the distance of a parcel of gas from the Galactic centre in a longitude and azimuth dependent manner [Eqn. (3)]. Therefore, averaging over azimuth also entails a radial averaging if the wrong rotation curve is adopted. This problem can be entirely circumvented if the data is gridded in the manner described by Eqn. (1), since every parcel of gas with the same W velocity is located at the same Galactocentric radius[§]. This gridding also guarantees that the inferred widths depend on the actual value of R_0, but are *independent* of Θ_0 and the Milky Way's rotation curve (Merrifield 1992).

However, Merrifield did not provide estimates for the errors on the flaring. In order to obtain such errors, we searched the literature for other determinations of the thickness of the Milky Way's gas layer. We found two other publications where both the thickness of the gas layer and Galactocentric azimuths were specified, so that these measurements could be converted to different values for R_0 and Θ_0. From Diplas & Savage (1991) we determined the full

§ This arguments only holds in the absence of non-circular motions. The gaseous velocity dispersion ensures that the gas arises from a range in radii.

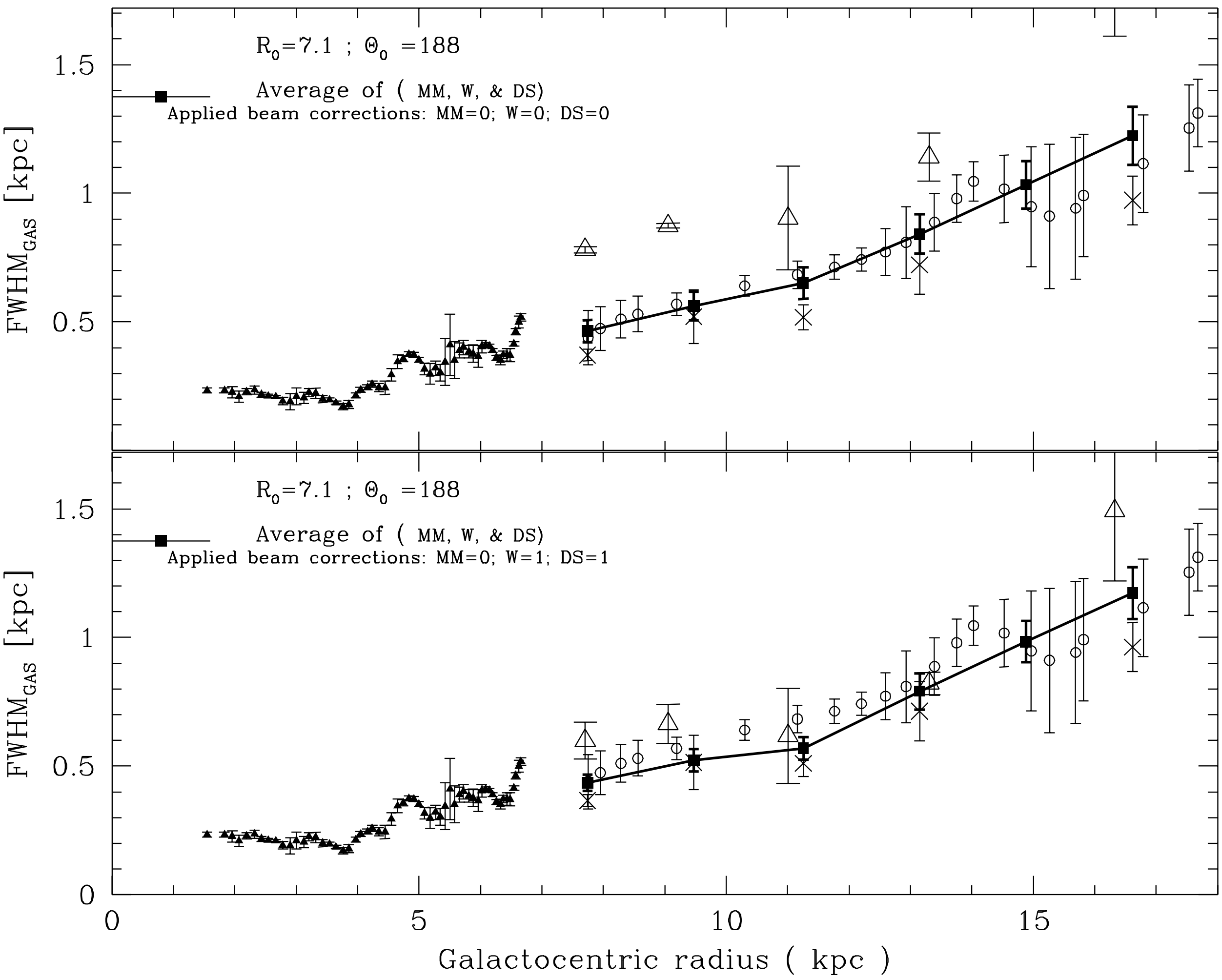

Figure 3. The thickness of the H I layer of the Milky Way (R_0=7.1 kpc, Θ_0=188 km s^{-1}). The widths in the inner Galaxy were taken from Malhotra (1995). For the outer Galaxy, we plot the widths from Diplas & Savage (1991; open triangles), Wouterloot *et al.* (1992; crosses), Merrifield (1992; open circles), and the average (thick full line & filled squares). The top panel represents the "raw" measurements, in bottom panel we present the beam-size corrected widths. From this figure we estimate the thickness of the H I layer at the solar circle to be 410 ± 30 pc. Similarly, we find $\mathrm{FWHM}_{\mathrm{H}_2}(R_0) = 141 \pm 20$ pc.

widths at half maximum (FWHM) at three azimuths, and from Wouterloot *et al.* (1990) we extracted measurements at eight positions. These 11 measurements were re-gridded on a common distance scale and averaged with the determination by Merrifield (1992). We gave Merrifield's data double weight because his values reflect an average over 360 degrees in azimuth. The results are presented in the top panel of Fig. 3. There is a large and systematic difference between the results of the various authors. These differences can be attributed to the effects of the beam-size on the observations, which affect different azimuths to a different degree. After correcting for the beam effect¶, the 12 observations at each Galactocentric distance are in far better agreement, and are distributed in a close to gaussian manner. We could thus determine the statistical average of the gas layer widths, and the errors thereupon (Fig. 3, bottom panel).

¶ The Diplas & Savage data had to corrected with a variable beam size as the Bell Lab's survey they used (Stark *et al.* 1991) was undertaken on a $\alpha - \delta$, rather than a $l - b$ grid. For the Wouterloot *et al.* data the appropriate beam size was used for each of their two surveys. The Merrifield data was not corrected for beam-size as the widths were determined by a fit to the full range in azimuths.

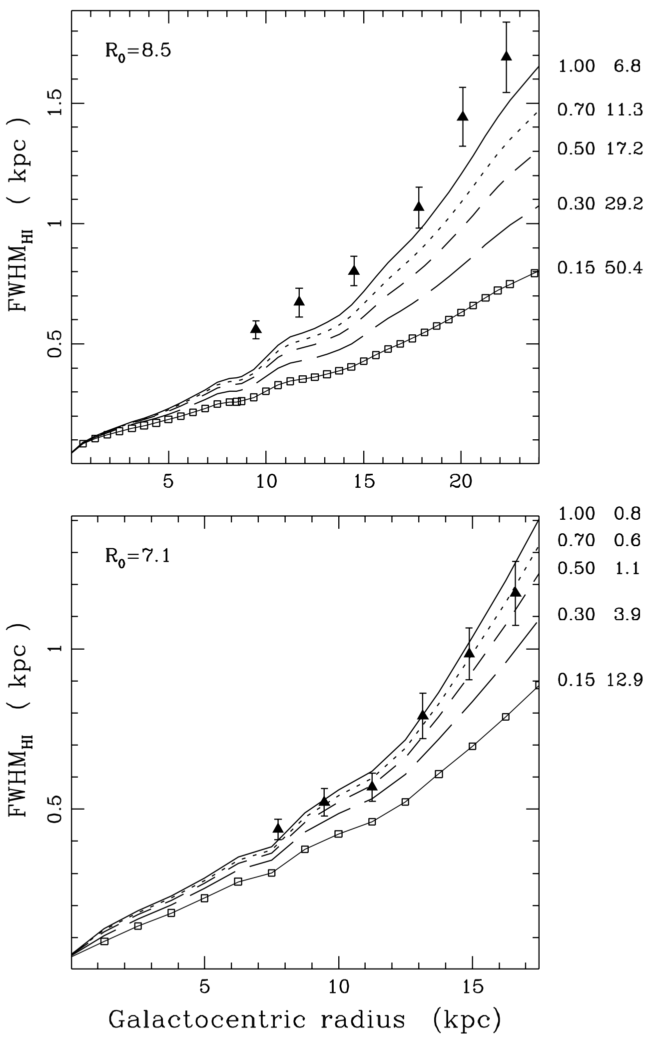

Figure 4. The observed flaring of the Galaxy's gas layer (triangles) compared with the flaring predicted for a number of mass models that reproduce the observed rotation curve and Σ_*. The models in the top panel have been calculated assuming R_0 =8.5 kpc and stellar mass-to-light ratio $\Upsilon_{*,\mathrm{K-band}}$ = 0.53; the bottom panel shows models with R_0 =7.1 kpc and $\Upsilon_{*,\mathrm{K-band}}$ = 0.70. The models shown here have a disk scale-length of 2.5 kpc; other relevant model parameters can be found in table 1 of paper II. The flattening of the model and the reduced χ^2 value of the fit is shown for each case. Note that, as discussed in the text, the flaring depends on the adopted rotation curve, since the distance to different parts of the gas is itself calculated from the rotation curve.

4.2 The physical state of the ISM beyond the optical disk

In the Introduction we mentioned that the ISM beyond the optical disk is likely to be in the warm neutral phase. At this point we like to further substantiate this statement. Because the volume densities, pressures, metallicities and dust contents of the ISM all decrease with increasing Galactocentric distance, it becomes progressively more difficult to form molecular hydrogen. As a consequence, the H_2 column density decreases faster than the H I column density towards the outer regions, which is commonly observed in spiral galaxies. The Milky Way is no exception (eg. Olling & Merrifield 1998b, their Fig. 2). Furthermore, at low pressures it is not possible to maintain a two phase medium (Maloney 1993; Wolfire *et al.* 1995) so that one expects that the cold neutral medium (CNM) is no longer a constituent of the ISM. Braun and collaborators (1992, 1997, 1998) describe an extensive network of high H I surface brightness features which they identify with the cold neutral medium. Furthermore, Braun (1997, 1998) finds that the CNM disappears when the B-band surface brightness falls below the 25^{th} magnitude per square arcsec level. Thus, the CNM disappears in the outer parts of the stellar disk, and is all but absent beyond the stellar disk. These observations corroborate the theoretical expectation that the warm neutral phase dominates at large galactocentric distances. Furthermore, at these large distances star formation has all but ceased to exist, so that the myriad structures thought to be associated with energy input from dying stars like worms, bubbles, holes, chimneys etc. are expected to be rare exceptions beyond the optical disk. Sensitive, high resolution H I spectral line observations show that the velocity profile is well represented by a single gaussian function (Olling 1996b), indicating that a single temperature component describes the H I well.

The ionized fraction of the ISM is expected to decrease with distance as it is closely associated with sites of star formation (eg; Ferguson *et al.* 1996; Wang, Heckman & Lehneert 1997). Furthermore, the ionizing effects of the extra-galactic background radiation field on the gas layer only become important at very large radii where the H I column density falls below about 1 $M_\odot$ pc^{-2} (Maloney 1993; Dove & Shull 19944; Olling 1996c).

In summary, observational and theoretical evidence indicates that the interstellar medium beyond the optical disk is in the warm neutral phase, with low molecular and ionized fractions. The medium can thus be described as a single, iso-thermal component.

4.3 Comparing predictions and observations

Given a potential, it is straightforward to determine the thickness of such an iso-thermal medium from the equation of hydrostatic equilibrium (Olling 1995; Olling 1996b; Paper II). For the moment we assume that non-thermal pressure gradients associated with magnetic fields and cosmic rays (Kulkarni & Heiles 1988) do not contribute to the hydrostatic balance. Furthermore we assume that the H I has a velocity dispersion of 9.2 km s^{-1} as observed in the inner Galaxy (Malhotra 1995). However, the exact value of the gaseous velocity dispersion and the amount of non-thermal pressure support of the gas layer are of critical importance when inferring the vertical force law from the observed gas layer widths. We address these issues in detail in the accompanying paper (Paper II), where we find that the effective gaseous velocity dispersions must be close to the default value of 9.2 km s^{-1} and that the conclusions we reach in this paper on the values of the Galactic constants, the mass of the stellar disk and the dark halo's flattening are not significantly altered.

In order to see how well models can reproduce the observed flaring of the gas layer, we have calculated several tens of mass models. Fig. 4 shows the results for two sets of models. Clearly, no dark halo can reproduce the observed flaring for the model with $R_0 = 8.5$ kpc, while the model with $R_0 = 7.1$ kpc fits the observed flaring even down to the inflection at ~ 12 kpc in the data. Note that the gaseous self-gravity is very important: not incorporating its effects would increase the model gas layer widths by up to 50%. Combining the ensemble of simulations, we find that acceptable fits can only be found with $q \geq 0.5$, and that the best fits occur for models with the shortest values of R_0 adopted. These models also have the flattest dark halos.

5 COMBINING CONSTRAINTS ON THE HALO'S FLATTENING

For all models considered we have calculated the flattening inferred from the amount of dark matter close to the plane ($q_{1.1}$) and the flaring of the gas layer ($q_{\rm H\,I}$). As mentioned in the Introduction, $q_{1.1}$ depends on the adopted mass of the stellar disk (Σ_*): if Σ_* is small, then there must be a larger contribution to the total mass near the plane from the dark halo, and so the halo must be flatter ($q_{1.1}$ smaller). On the other hand, $q_{\rm H\,I}$ is virtually independent of Σ_* since $q_{\rm H\,I}$ depends on the properties of the halo at large radii, where the effects of the disk are negligible. Self-consistency requires that there is a region of $\Sigma_* - q$ parameter space where both methods yield identical results. In Fig. 5 we show these effects for one combination of the Galactic constants. For other assumed values of R_0 and Θ_0 the behavior is similar: the slopes of the $q_{\rm H\,I}$ and $q_{1.1}$ lines are rather different, and their intersection gives the values for Σ_* and q where the flaring gas layer method and the stellar kinematical determination of $\Sigma_{1.1}^{tot}$ are mutually consistent. However, the location of the intersect depends on the assumed values of the Galactic constants.

5.1 Different Galactic constants

Because of our location inside the Milky Way, the observed linear thickness of the gas layer depends on the adopted values for Θ_0 and R_0, while the thickness predicted by the models depends on the dark matter density, and hence on Θ_0. Similarly, from equation (1) we infer that the shape of the rotation curve, and hence the halo parameters and $q_{1.1}$, are a function of both R_0 and Θ_0.

We have therefore repeated the above analysis for the full range of possible values for R_0 and Θ_0. For each combination of Galactic constants it is straightforward to determine the dependence of $q_{1.1}$ on Σ_* from a series of mass models with different halo flattening and stellar disk masses.

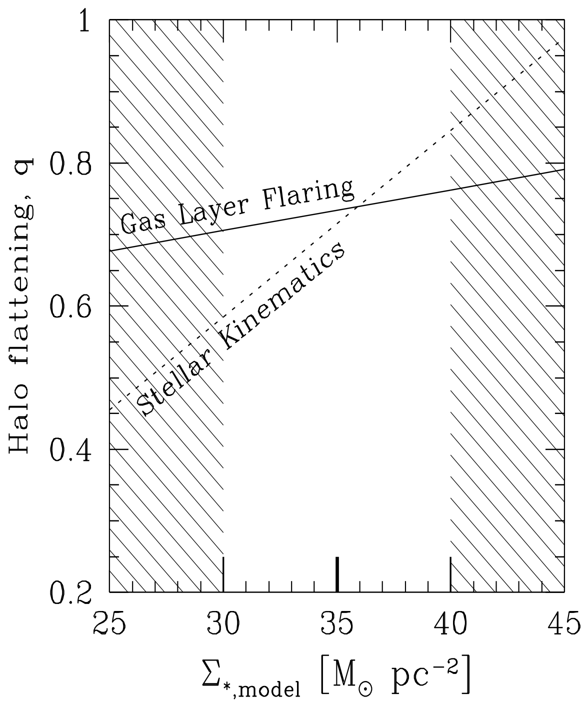

Figure 5. The inferred flattening of the Galactic halo, q, as a function of the adopted column of stellar disk mass in the Solar neighborhood, Σ_*. We show the best fits to the stellar kinematic constraints (dotted line) and the flaring of the H I layer (full line). The shaded region shows values of Σ_* that lie more than 1-σ from the observed value. Consistency requires that the two methods yield identical halo flattenings and stellar column densities: the intersection of the two lines yields these values for q and Σ_*. These calculations have been made for $R_0 = 7.1$ kpc and $\Theta_0 = 189$ km s^{-1}. For models with different values of the Galactic constants, the flaring and stellar kinematics lines, as well as their intersect will be located in another region of parameter space.

Models with different disk scale-lengths follow the same $q_{1.1}(\Sigma_*)$ relation.

However, in order to obtain the constraint due to the H I flaring, one needs to perform a full integration over the Galactic density distribution to obtain the vertical force law and hence the hydrostatic equilibrium thickness. Such an operation would be computationally very expensive. Therefore, we adopt an approximation to determine the model gas layer widths (see Paper II). Unfortunately, this approximation is only sufficiently accurate beyond the truncation of the stellar disk, so that typically half the flaring measurements are rendered useless. Given the scarcity of the data points, we determine the best fitting halo flattening by Monte Carlo simulation. In each realization i of the comparison of the model and observed widths, we draw an "observation" from a gaussian distribution with a mean and dispersion equal to the observed width and observational error, respectively. For each trial i we then determine χ^2 by summing over all "observations" j: $\chi_i^2(q) = \sum_j \left((W_{j,mod}(q) - W'_{j,obs})/\Delta W_{j,obs}\right)^2$, with $W_{j,mod}(q)$ the gas layer width for the model with flattening q, $\Delta W_{j,obs}$ the observed error, and $W'_{j,obs}$ the randomly drawn "observed" thickness. The best fit value, q_i, is determined from a quadratic fit to the $\chi_i^2(q)$ values close to the minimum. The distribution of the q_i's is approximately gaussian, and our final best fit value for $q_{\rm H\ I}$ is the average of 80 determinations of q_i, while the error equals the dispersion of the distribution of the 80 q_i's.

There is one complication that needs to be resolved. From Fig. 4, it is clear that there are some combinations of Galactic constants for which no oblate halo model will fit the observations. As mentioned in the Introduction, dark halos in which galaxies have formed
are likely to be oblate. We will therefore not pursue the prolate case in great detail. Instead, we note that the halo densities will change continuously beyond $q = 1$. To determine $q_{\rm H\ I}$ and $q_{1.1}$ in the prolate case, we apply the relations presented in Paper II to extrapolate into the prolate regime.

Now we are ready to determine Σ_* and q as a function of R_0 and Θ_0. For each R_0-Θ_0 combination, and for a range stellar mass-to-light ratios we determine the Σ_* and q values for which the flaring and stellar kinematical constraints are mutually consistent, in the same manner as displayed in Fig. 5. The thus-determined values are contoured in Fig. 6. It is straightforward to understand the behaviour displayed in this figure. Since the model thickness of the gas layer is inversely proportional to the dark matter density (Olling 1995; Olling 1996b; Paper II), a rounder, more tenuous halo is required as the amplitude of the rotation curve increases, so that q increases with Θ_0. Because of the kinematic nature of the distance determinations of the gas, the physical thickness of the gas layer increases with R_0 at any given Θ_0. Thus, with increasing R_0, lower dark matter densities are required for the model widths to match the observed flaring. Since we have just shown that the halo flattening is fixed by the amplitude of the rotation curve, the only way to decrease the DM densities and simultaneously retain the same rotation curve, is by having a more "maximal" disk, ie, by increasing Σ_*. Hence the observed increase of Σ_* with R_0. The results of this analysis for Σ_* depend somewhat on the choice for the mass-to-light ratio of the bulge ($\Upsilon_{\rm B}$). We have therefore repeated the procedure for several values of $\Upsilon_{\rm B}$ (0.4, 0.5, 0.6, and 0.7, in the K-band) and averaged the outcomes before calculating the results displayed in Fig. 6. We find no systematic trend with $\Upsilon_{\rm B}$.

If we require that the dark halo is oblate, then

$$\Theta_0 \quad \lesssim \quad 188 - 5.55(R_0 - 7) + 4.01(R_0 - 7)^2 \,. \qquad (4)$$

We thus eliminate Milky Way models with $\Theta_0 \gtrsim 190$ km s^{-1} for all but the smallest R_0 values. In the oblate region of parameter space, and for $R_0 \gtrsim 6.5$ kpc, the stellar column density and halo flattening contours are almost perpendicular. In this region, Θ_0 constrains q and vice versa, while Σ_* and R_0 constrain each other almost independent of Θ_0.

To summarize, unless the stellar disk is very light or our distance to the Galactic centre is very small, the Milky Way's dark matter halo must be close to spherical.

5.2 The Oort Functions

So far, we have not considered constraints imposed by the values of the Oort constants, A and B, individually. Both Oort constants are obtained from $\Theta(R)/R$ and the gradient of the rotation curve. Thus, the Oort *functions* $A(R)$ and $B(R)$ can be used to place limits on the Galactic constants. Such an analysis is insensitive to the actual mass of the stellar disk and the shape of the halo, and is thus essentially independent of the work presented in this paper.

We recently completed such a detailed analysis of the Oort functions (Olling & Merrifield 1997a,1998b). In that paper, we extended previous work by carefully addressing the radial variation of the Oort functions, and including a realistic radial distribution of the interstellar gas. We found strong evidence for a leaner Milky Way: $R_0 = 7.1 \pm 0.4$ kpc, and $\Theta_0 = 184 \pm 8$ km s^{-1}. The cross in Fig. 6 represents the Galactic constants determined from the Oort functions.

6 CAVEATS

With the release of ESA's Hipparcos catalogue (Perryman *et al.* 1997), many new possibilities arise for the accurate determination of the Galactic constants and stellar column density. Also, VLBA proper motion measurements of Sgr A* hold promise to accurately determine the Galactic constants (Reid 1998). Of course, it is possible that it will turn out that the true values of the Galactic constants are incompatible with the results we present in Fig. 6. If so, we will have to reconsider our choice for the radial distribution and shape of the dark matter, and learn more about the Milky Way's dark matter distribution. However, in our analysis we have made a number simplifying assumptions, each of which will be violated to some degree in the real Milky Way galaxy. In order to gain a deeper understanding of the Galactic dark matter distribution, the importance of these effects will have to be gauged. For example, since the Sun is located in an interarm region, it is not entirely clear to what extend the total column density of matter as determined in the Solar neighborhood (Kuijken & Gilmore 1991) is representative of the average column density at our Galactocentric radius. In addition, the standard interpretation of radial and proper motions in the Milky Way may be an over simplification, as the Galaxy may not be axisymmetric (Kuijken & Tremaine 1994, and references therein). Furthermore, it is possible that the gas layer of the Milky Way is not in equilibrium, as the presence of the warp may indicate. A final potentially-serious shortcoming is our neglect of the non-thermal contribution to the energy density of the ISM.

The question of the equilibrium of the Galactic H I layer can be addressed by applying Merrifield's techniques (1992) to the superior quality and extent of the Leiden-Dwingeloo survey of the northern hemisphere (Hartmann & Burton 1997). Preliminary analysis indicates that the Milky Way's warp is much more regular than previously thought. The issue of the non-thermal pressure contribution and the related uncertainty in the gaseous velocity dispersion can be resolved already. In Paper II we show that significant non-thermal pressure support of the gas layer is in conflict

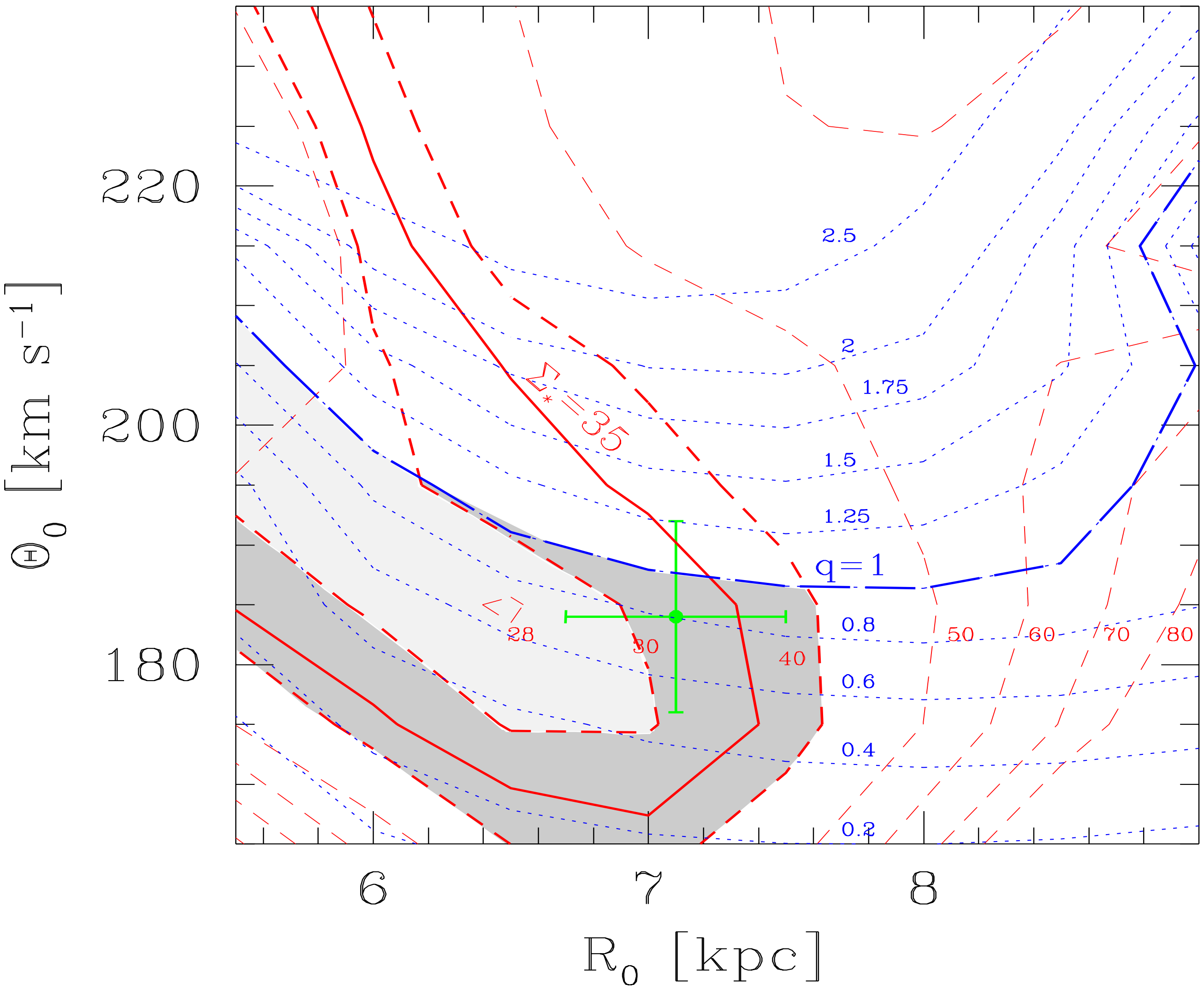

Figure 6. Here we present the *mutually consistent* set of Galactic constants, stellar column density in the Solar neighborhood (Σ_*; long dashed lines) and halo flattening (q; dotted lines). The oblate-prolate boundary is indicated by the heavy dash-dotted line. The heavy full line and the heavy dashed line corresponds to KG89's determination of Σ_*, and the $\pm 1-\sigma$ values. The upper limit of GBF97's determination of the stellar column density corresponds to the $\Sigma_* \sim 30\ M_\odot\,\mathrm{pc}^{-2}$ contour. In the shaded region of parameters space, the dark halo is oblate and the mass of the stellar disk as measured (dark shading denotes the KG89 stellar mass range, light shading is used for GBF97's Σ_* range). The lowest column density ($\sim 27.5\ M_\odot\,\mathrm{pc}^{-2}$) is found for $(R_0, \Theta_0) \sim (6.5, 185)$. Both the halo flattening and stellar column are determined to $\sim 6\%$ accuracy. Because the Galactic constants, Σ_*, and q are mutually consistent one cannot arbitrarily choose the four parameters. Fixing one of the four parameters severely restricts the other three. Any two parameters follow immediately from any choice of the other two. The fat cross located at (R_0, Θ_0)= (7.1 kpc, 184 km s^{-1}) represents our determination based on the Oort constants (Olling & Merrifield 1997a,1998b), which is entirely independent of, but fully consistent with the analysis presented here.

with the observational constraint on the local stellar column density for all but the smallest values of R_0.

7 THE GALACTIC MASS

A more slowly rotating Milky Way might be expected to be less massive as well, since Mass(R) $\propto R \times \Theta(R)^2$. The Galactic mass is constrained by the space motions of tracers that reach far from the centre of the Galaxy, such as high velocity stars, the Milky Way's satellites, and M31. From Carney, Latham & Laird (1988), we find that the inferred local escape velocity is almost independent of the assumed value for Θ_0. In terms of the Galactic mass models discussed by Fich & Tremaine's (1991), the observed local escape velocity is consistent with Θ_0-values between 180 and 220 km s^{-1}. In a more detailed analysis, Kochanek (1996) finds that a large range in halo truncation radius and halo rotation speed (v_c) is allowed if only high velocity stars, the Galactic satellites and M31 are considered. Kochanek also finds that by far the strongest constraint on the halo's rotation speed at large distances is set by the amplitude of the inner Galactic rotation curve, and that $v_c \sim \Theta_0$ out to large radii (as in external galaxies).

The "Local Group timing" argument (Kahn & Woltjer 1959; Kochanek 1996, and references therein) provides the connection between the halo's radial extend and rotation speed. It is assumed that M31's peculiar velocity is the result of the gravitational interaction between the Milky Way and M31 only. Thus, M31's radial velocity constrains the total mass of both galaxies. In Kochanek's model, the mass of the Milky Way is not infinite because the Galactic dark halo is truncated at radius r_j, so that the total mass is proportional to $r_j \times {v_c}^2 (\sim r_j \times \Theta_0^2)$. Since the total mass is given by M31's observed peculiar velocity[‖], it follows that a more slowly rotating Milky Way requires a more extended dark halo. Specifically, if we consider two kinematic models for the Milky Way, one with $v_c = \Theta_0$, and the other with $v_c = \Theta_0 + \Delta\Theta_0$, Kochanek's (1996) equations (12) - (14) imply the following relation for the truncation radii:

$$r_j(\Theta_0 + \Delta\Theta_0) \approx r_j(\Theta_0)\left[1 - \frac{1}{3}\frac{\Delta\Theta_0}{\Theta_0}\right] . \qquad (5)$$

Thus, any choice of Θ_0 is consistent with M31's velocity as long as r_j does not exceed the Milky Way's tidal radius. Thus, if the halo's truncation radius is about 210 kpc, a Galactic rotation speed of 184 km s^{-1} is fully consistent with the constraints imposed by high velocity stars, the orbits of the Galactic satellites and M31's orbit. This halo radius is indeed smaller than the Milky Way's tidal radius [375 kpc, (Kochanek 1996)], and compares well with the extend of the Milky Way's satellite system and the halo sizes inferred for external galaxies (Zaritsky *et al.* 1997). Thus, the mass of the Milky Way need not be affected by modest changes in the Galactic constants.

7.1 Dark Matter in the Solar Neighborhood

Kuijken & Gilmore (1989) found no evidence for a substantial amount of dark matter in the Solar neighborhood. This result is further corroborated by a recent Hipparcos-based determination of the local volume density of matter by Crézé *et al.* (1998). Their value of $\rho_{tot}(R_0) = (76 \pm 15)\ 10^{-3}\ M_\odot\ \mathrm{pc}^{-3}$ is substantially smaller than previous determinations, and, after subtraction of the stellar and ISM densities (Paper II), there is only room for a very small amount of dark matter indeed [$\rho_{DM}(R_0)$ = (-10 ± 15) $10^{-3}\ M_\odot\ \mathrm{pc}^{-3}$]. Our models indicate that this low local density of dark matter is only possible for small values of the Galactic constants, and an almost round dark matter halo.

‖ M31's peculiar velocity with respect to the Galactic centre is hardly influenced by the magnitude of Θ_0.

8 THE CASE FOR A LEANER MILKY WAY

With the evidence in this paper pointing to a smaller, slower-rotating Milky Way than is customary assumed, we must re-consider the evidence which has been used to derive the established values of R_0 = 8.5 kpc, and Θ_0 = 220 km s^{-1}.

8.1 Determining Θ_0

To our knowledge, there is no reliable direct determination of the local Galactic rotation speed and its error. In §7 we discussed the methods based on the kinematics of distant tracers of the Galactic potential, and the fact that they do not constrain Θ_0 very strongly. The value for Θ_0 inferred from more local data depends to a large extend on which auxiliary assumptions are made. For example, assuming a locally flat rotation curve, the tangent point data in the inner Galaxy yields 220 ± 20 km s^{-1} (Gunn, Knapp & Tremaine 1979). From similar data, Rohlfs *et al.* (1986) find Θ_0 = 184 ± 12 km s^{-1}, when assuming $B/(B-A)$=0.42, and Merrifield (1992) finds Θ_0 = 180 ± 20 km s^{-1} if the Milky Way is similar to other Sb and Sc galaxies in terms of rotation speed and rotation curve gradient.

8.2 Determining R_0

The methods used in the determination of the "large" value for R_0 can be segregated into several calibration groups based on kinematical models of the Milky Way and the distribution of standard candles. The various methods to determine R_0 have been extensively reviewed by Reid (1993). Before discussing the standards candle results (§8.2.2), we briefly review the kinematical methods.

It is important to note that some of Reid's (1993) calibration groups ("Scaled by Θ_0 = 220 km s^{-1}", "Using Oort's Constants", "OB Star Calibration") are based on uncertain kinematic properties of the Galactic disk. For example, all methods assuming Θ_0 = 220 km s^{-1} are fully consistent with our small value of R_0 after re-scaling to Θ_0 = 184 km s^{-1}. The "Using Oort's Constants" and "OB Star Calibration" methods depend on the value for the Oort constant A, and the inferred R_0 scales directly with the adopted value of A. Using these calibration methods, a smallish Oort A constant as inferred from the Lick Northern Proper Motion Survey (Hanson 1987) yields $R_0 \sim 7$ kpc. However, the currently accepted values for Θ_0 and A are subject to significant observational and systematic uncertainties.

8.2.1 Determining the Oort constants

In their review of the Galactic constants, Kerr & Lynden-Bell (1986) stressed that "it is important to state the range of distances of the stars used in any determination of the Oort constants". It now appears that, when interpreting radial and proper motions, not only are the distances to the stars used crucial, but their Galactocentric radii are also important (Olling & Merrifield 1998b).

Generally, the radial variation of the Oort functions has not been taken into account, so that the observational determination of the Oort constants may be strongly affected by systematic errors. Thus, the Galactic constants determined using the Oort constants may be compromised. In our analysis of the Oort constants (Olling & Merrifield 1998b) we find that the Oort constants as determined in the solar neighborhood and the distant Galaxy differ significantly. We argue that this difference is the result of the ISM's non-monotonic contribution to the rotation curve (see Fig. 2). Such a difference could also arise from substantial non-circular motions in the solar neighborhood. Evidence to that effect comes from two recent analyses of radial velocities (Pont, Mayor & Burki 1994) and proper motions of distant Cepheids (Feast & Whitelock 1997) in which the second and third order derivatives of the local rotation curve are determined: the proper motion and radial velocity solutions for the 2^{nd} and 3^{rd} order derivatives differ by 3.9σ and 1.3σ, respectively. However, our Galactic models – which include a locally non-linear rotation curve and assume circular motions – predict the radial and proper motions of both nearby stars and distant Cepheids correctly, as well as the Oort constants (Olling & Merrifield 1998b). Furthermore, our rotation curve models predict a 40% difference in the Oort constants as determined in the inner and outer Galaxy and extrapolated to the Solar circle (Olling & Merrifield 1998b). This prediction compares well with the ratio of the Oort constants A as determined from H I data for the inner and outer Milky Way [1.4 ± 0.24; (Merrifield 1992)].

At any rate, it is likely that non-circular motions as well as a non-monotonic mass distribution complicate the interpretation of radial and proper motions, so that the determination of the Galactic constants based on the Oort constants may be unreliable.

8.2.2 R_0 from Standard Candles

Another way to determine the distance to the Galactic centre is based on the spatial distribution of standard candles, such as RR-Lyra stars, Cepheids, globular clusters, horizontal branch stars, or red giants (Reid 1993). Due to the uncertain metallicity dependence of the absolute magnitudes of these tracers, the results have not been conclusive. For example, the distance to Galactic centre based on RR-Lyrae varies between 6.9 ± 0.6 and 8.7 ± 0.7 kpc (Reid 1993). Hipparcos parallaxes could settle the metallicity issue. However, new, unexplained systematics are starting to appear. For example, Reid (1998) studied five globular clusters and found a 17% difference between M5's distance based on main sequence fitting and RR-Lyrae absolute magnitudes. Reid suggests that this difference could arises as a result of different helium abundances. A discrepancy of similar magnitude is found when the Pleiades' Hipparcos distance is compared with ground based methods and distances to other open clusters. Soderblom *et al.* (1998) argue that this discrepancy is not the result of composition effects, but rather that Hipparcos' Pleiades distance is wrong.

A recent study that takes the RR-Lyrae metallicity-magnitude relations into account yields a smallish value for R_0 of 7.6 ± 0.4 kpc (Layden *et al.* 1996). Other "standard candle" methods yield rather big R_0's: for example, with the re-calibration of the Cepheid distance scale, Feast & Whitelock (1997) find $R_0 = 8.5 \pm 0.5$ kpc, and "red clump" stars yield 8.5 ± 0.4 kpc (Paczyński & Stanek 1997). However, it should be kept in mind that the Cepheid-based R_0-determination is based on a kinematical model for the Milky Way. As mentioned above (§8.2.1), a detailed analysis of the radial behavior of the Oort functions shows that a small distance to the Galactic centre is consistent with both the radial velocities and proper motions of Cepheids (Olling & Merrifield 1998b).

We have two concerns with regard to the "red clump" method. Since both RR Lyra stars and red clump stars are part of the horizontal branch, the objects forming the red clump are subject to similar uncertain metallicity corrections as RR Lyra stars. Possible evidence of a "second parameter" effect is visible in the Hipparcos colour-magnitude diagram of the red clump stars (Paczyński & Stanek 1997; Stanek & Garnavich 1998),which shows significantly different averages and slopes in the M_I distributions in the $(V\text{-}I)_0 \in [0.8,0.95]$, $[0.95,1.1]$, and $[1.1,1.25]$ ranges. Furthermore, theoretical investigations show that the clump's morphology and absolute magnitude depend strongly on stellar mass, metallicity (Seidel, Demarque & Weinberg 1987) and star formation history (Cole 1998; Girardi *et al.* 1998), which – in the Solar neighbourhood – seem to cancel out to a large extend.

Above we discussed some of the systematics associated with several techniques that have been used to determine the Galactic constants, and in Section 6 we mentioned some of the systematics that can compromise the analysis presented in this paper. We conclude that – despite enormous research efforts over the last seventy years – the systematics involved in the determination of the Galactic constants are not well understood: systematic errors dominate. Therefore, the "current best" and IAU values of the Galactic constants are really "consensus averages." As a result, the quoted uncertainties are not errors in the statistical sense, so that they cannot be used to exclude regions of parameter space with any degree of significance.

9 SUMMARY AND CONCLUSIONS

To date, the observational uncertainties in the distance to the Galactic centre (R_0), the Galactic rotation curve, the mass of the stellar disk (Σ_*), and the large scale photometry allow for a substantial range in the Galactic DM halo's shape (q). This uncertainty is largely due to the absence of tracers that constrain the DM density. In this paper, we seek to remedy this situation by incorporating the limits set by two independent methods: 1) the stellar kinematics in the Solar neighborhood, and 2) the radial variation of the thickness of the H I layer beyond $\sim 1.5 R_0$. Each method on its own does not provide enough information to greatly improve our knowledge of the dark matter density distribution, but the combination of the two techniques narrows the range substantially. Both methods place limits on the axis-ratio of the dark matter halo. The value of q inferred from the stellar kinematics depends strongly upon the mass of the stellar disk. However, when combining the constraints set by the H I flaring and stellar kinematics methods, we find that the uncertain parameters (R_0, Θ_0, Σ_*, q) are strongly interrelated. In fact, an accurate determination of any two of these four parameters uniquely determines the remaining two. Thus, the parameters of an internally consistent Galaxy model have to be chosen with care. For example, the IAU standard values of $R_0 = 8.5$ kpc, and $\Theta_0 = 220$ km s^{-1} (Kerr & Lynden-Bell 1986) imply Σ_*=53.4 $M_\odot$ pc^{-2} and $q = 1.85$, and the current best estimates of $R_0 = 7.8$ kpc and $\Theta_0 =$ 200 km s^{-1} yield Σ_*= 50.0 $M_\odot$ pc^{-2} and $q = 1.69$. Because the dark halo is likely to be oblate (Katz & Gunn 1991; Udry & Martinet 1994; Dubinski 1994), such large values for the Galactic constants are essentially excluded. In principle, the constraints provided by the H I flaring method are sensitive to the adopted value for the gaseous velocity dispersion. In Paper II we show that the gaseous velocity dispersion in the outer Galaxy cannot differ substantially from the measured value in the inner Galaxy. This analysis also excludes a significant non-thermal pressure support of the gas layer.

A significantly flattened dark matter halo is only possible if the local rotation speed is smaller than about 170 km s^{-1}. If Θ_0 is any larger, decaying massive neutrinos (Sciama 1990) and disk-like cold molecular hydrogen (Pfenniger, Combes & Martinet 1994) are no longer viable dark matter candidates, as they require $q \lesssim 0.2$.

Small values for Galactic constants, $R_0 = 7.1 \pm 0.4$ kpc and $\Theta_0 = 184 \pm 8$ km s^{-1} have also recently been determined from an analysis of the Oort constants (Olling & Merrifield 1997a,1998b). These Galactic constants are entirely consistent with the results presented in this paper. Both sets of results imply a small amount of dark matter in the Solar neighborhood with a density of 6.6 10^{-3} $M_\odot$ pc^{-3}, or 0.25 GeV/c^2 per cubic centimetre, an almost round dark matter halo ($q \sim 0.8$), and a stellar column density of $\sim$32 $M_\odot$ pc^{-2}. These results indicate that the galaxy we live in is somewhat smaller than commonly thought. Because the values for the Galactic constants found in the literature are *consensus averages* with *consensus* error estimates, it is not possible to determine the significance level at which our estimates differ from the IAU-recommended or 'current bets' values. A small Galaxy is also implied by the only geometric distance determination to the Galactic centre based on the proper motions of water masers, which yields $R_0 = 7.2 \pm 0.7$ kpc (Reid 1993).

It is expected that in the near future much more accurate determination of R_0, Θ_0, and Σ_* will become available from new, high quality, databases such as Hipparcos. Since only two of these parameters are required to determine the dark halo's flattening, it will be possible to check the self-consistency of the models we have built here. The overdetermination of these mass models holds great promise for learning more about the Milky Way's dark matter distribution.

ACKNOWLEDGEMENTS

We thank Andy Newsam, Irini Sakelliou, Konrad Kuijken, Marc Kamionkowski, Jacqueline van Gorkom, and the referee for useful discussions.

REFERENCES

Arnaboldi M., Capaccioli M., Cappellaro E., Held E.V., Sparke L.S., 1993, A&A, 267, 21
Bahcall J.N., 1984a, ApJ, 276, 156
Bahcall J.N., 1984b, ApJ, 276, 169
Bahcall J.N., 1984c, ApJ, 287, 926
Becquaert J.F., Combes F., Viallefond F. 1997, A&A, 325, 41
Begeman K., 1989, A&A, 223, 47
Binney J.J., Jiang I.G., Dutta S., 1997, submitted to MNRAS (astro-ph/9708024)
Bosma A., 1981, AJ, 86, 1825
Brand J. & Blitz L., 1993, A&A, 275, 67
Braun R., 1998, in Franco J., Carraminana A., eds, Interstellar Turbulence, Proceedings of the 2nd Guillermo Haro Conference, Cambridge University Press.
Braun R., 1997, ApJ, 484, 637
Braun R., Walterbos R.A.M., 1992, ApJ, 386, 120
Bronfman L., Cohen R.S., Alvarez H., May J. & Thaddeus P., 1988, ApJ, 324, 248
Broeils A., 1992, Ph. D. Thesis, University of Groningen
Buote D.A., Canizares C.R., 1998, to appear in MNRAS, astro-ph/9803208
Buote D.A., Canizares C.R., 1996, ApJ, 468, 184
Carney B.W., Latham D.W. & Laird J.B., 1988, AJ, 96, 560
Cole A.A., 1998, Accepted for publication in ApJL
Combes F., 1991, ARA&A, 29, 195
Crézé M., Chereul E., Bienaymé O., Pichon C., 1998, A&A, 329, 920
Dehnen W., Binney J., 1998, MNRAS, 294, 429
Diplas A. & Savage D.S., 1991, ApJ, 377, 126
Dove J.D., Shull J.M., 1994, ApJ, 423, 196
Dubinski J., 1994, ApJ, 431, 617
Dubinski J., Kuijken K., 1995, ApJ, 442, 492
Feast M., Whitelock P., 1997, MNRAS, 291, 683
Ferguson A.M.N., Wyse R.F.G., Gallagher J.S., Hunter D.A., 1996, AJ, 111, 2265
Fich M., Tremaine S., 1991, ARA&A, 29, 409
Girardi L., M. A. T. Groenewegen M.A.T., Weiss A., Salaris M., 1998, submitted to MNRAS (astro-ph/9805127)
Gould A., Bahcall J.N., Flynn C. 1997, ApJ, (GBF97)
Gunn J.E., Knapp G.R., Tremaine S.D., 1979, AJ, 84, 1181
Hanson R.B., 1987, AJ, 94, 409 (H87)
Hartmann D., Burton W.B., 1997, "Atlas of Galactic neutral Hydrogen" Cambridge University Press
Hofner P. & Sparke L., 1994, ApJ, 428, 466
Kahn F.D., Woltjer L., 1959, ApJ, 130, 705
Katz N., Gunn J.E., 1991, ApJ, 377, 365
Kent S.M., 1987, AJ, 93, 816
Kerr F.J., Lynden-Bell D., 1986, MNRAS, 221, 1023
Kochanek K., 1996, ApJ, 457, 228
Kuijken K., Tremaine S., 1994, ApJ, 421, 178
Kuijken K. & Gilmore G., 1991, ApJ, 367, L9 (KG91)
Kuijken K. & Gilmore G., 1989b, MNRAS, 239, 605 (KG89)
Kuijken K. & Gilmore G., 1989a, MNRAS, 239, 571

Kulkarni S.R., & Heiles C., 1988, in Verschuur G.L., Kellermann K.I., eds, Galactic and Extragalactic Radio Astronomy, p. 95
Lake G., Feinswog L., 1989, AJ, 98, 166
Layden A.C., Hanson R.B., Hawley S.L., Klemola A.R., Hanley C.J., 1996, AJ, 112, 2110
Malhotra S., 1995, ApJ, 448, 138
Malhotra S., 1994, ApJ, 443, 687
Maloney P., 1993, ApJ, 414, 41
Merrifield M.R., 1992, AJ, 103, 1552
Nelson R.W., Tremaine S., 1995, ApJ, 442, 492
Olling R.P., Merrifield M.R., 1998a, MNRAS, qqq, qqqq (Paper II)
Olling R.P., Merrifield M.R., 1998b, MNRAS, 295, 737 (astro-ph/9802034)
Olling R.P., Merrifield M.R., 1997a, in the proceedings of the Santa Cruz' "Galactic Halos" workshop, astro-ph/9711157
Olling R.P., Merrifield M.R., 1997b, in the proceedings of the Santa Cruz' "Galactic Halos" workshop, astro-ph/9710224
Olling R.P., 1997c, p. 46, In the proceedings of "Aspects of Dark Matter in Astro- and Particle Physics", Heidelberg, September 1996 (World Scientific: Eds. H.V. Klapdor-Kleingrothaus, Y. Ramachers) *astro-ph/9612018*
Olling R.P., 1996b, AJ, 112, 481-490
Olling R.P., 1996c, AJ, 112, 457-480
Olling R.P., 1995, AJ, 110, 591
Paczyński B. & Stanek K.Z., 1997, submitted to ApJL, astro-ph/9708080
Parker E.N., 1966, ApJ, 145, 811
Peebles P.J.E., 1993, "Principals of Physical Cosmology", Princeton University Press
Perryman M.A.C., *et al.* , 1997, A&A, 323, L49P, and references therein
Persic M., Salucci P., Stel F., 1996, MNRAS, 281, 27
Pfenniger D., Combes F., & Martinet L., 1994, A&A, 285, 79
Pont F., Mayor M., Burki G. 1994, A&A, 285, 415
Reid M.J., 1998, BAAS, 29, #97.06
Reid M.J., 1993, ARA&A, 31, 345
Rohlfs K., Chini R., Wink J.E. & Böme R., 1986, A&A, 158, 181
Rubin V.C., Ford W.K., Thonnard N., 1980, ApJ, 238, 471
Sackett P.D., 1997, ApJ, 483, 103
Sackett P.D. & Pogge R.W. in *Dark Matter*, edited by S.S. Holt, C.L. Bennet (AIP conference proceedings 336), 1995, p. 141
Sackett P.D., Rix H.W., Jarvis B.J. & Freeman K.C., 1994, ApJ, 436, 629
Sciama D., 1990, MNRAS, 244, 1
Seidel E., Demarque P., Weinberg D., 1987, ApJS, 63, 917
Soderblom D.R., King J.R.,Hanson R.B., Jones B.F., Fischer D., Stauffer J.R., Pinsonneault M.H., 1998, astro-ph/9801281
Stanek K.Z., Garnavich P.M., 1998, to be published in ApJL, astro-ph/9802121
Stark A.A., Gammie C.F., Wilson R.W., Bally J., Linke R.A., Heiles C., Hurwitz M, 1992, ApJS, 79, 77
Steiman-Cameron T.Y., Kormendy J. & Durisen R.H., 1992, AJ, 104, 1339
Udry S. & Martinet L., 1994, A&A, 281, 314
Albada T.S. van & Sancisi R., 1986, Phil. Trans. R. Soc. Lond. A., 320, 447
Wang J., Heckman T.M., Lehnert M.D., 1997, ApJ, 491, 114
Warren M.S., Quinn P.J., Salmon J.K., Zurek W.H., 1992, ApJ, 399, 405
Wolfire M.G., Hollenbach D., McKee C.F., Tielens A.G.G.M., Bakes E.L.O., 1995, ApJ, 443, 152
Wouterloot J.G.A., Brand J., Burton W.B. & Kwee K.K., 1990, A&A, 230, 21
Zaritsky D., *et al.* , 1997, ApJ, 478, 39